Indian Journal of Chemistry
Vol. 58A, December 2019, pp. 1302-1310

Crystal structure, thermal analyses, and acetate binding properties in Zinc(II) complex of a urea-functionalized pyridyl ligand

Zaiwen Yang[a,b,*], Shasha Sun[a], Yilong Liu[a], Xiangrong Liu[a,b,*], Shunsheng Zhao[a, b], Zhen Zhang[a], Xinjuan Chen[b], Zheng Yang[a,b] & Xiaodan Jia[a,b]

[a]College of Chemistry and Chemical Engineering, Xi'an University of Science and Technology, Xi'an 710054, Shaanxi, China
[b]Key Laboratory of Coal Resources Exploration and Comprehensive Utilization, Ministry of Land and Resources, Xi'an 710021, Shaanxi, China
E-mail: yzwxk@foxmail.com (ZY)/ liuxiangrongxk@163.com (XL)

Received 29 May 2019; revised and accepted 22 November 2019

A zinc(II) acetate complex with a urea-functionalized pyridyl ligand, $[ZnL_2(OAc)_2]\cdot 2H_2O$ (**1**) (**L** = *N*-(4-chlorophenyl)-*N'*-(4-pyridyl)urea), has been synthesized by the reaction of **L** with $Zn(OAc)_2\cdot 2H_2O$ under water-containing condition. X-ray single-crystal diffraction analyses reveal that 2-D sheetlike network structure has been formed by the urea $N{-}H\cdots N_{pyridyl}$ interactions and C–H···O interactions in the free ligand **L**. Complex **1** features 3-D hydrogen bonded network formed by intermolecular N–H···O hydrogen bonds and O–H···O hydrogen bonds involving urea groups, acetate anions and bridged water molecules. The hydrogen bonds play an important role in stabilizing the supramolecular structures. Thermal gravity analyses have been used to investigate the thermal stabilities of **L** and **1**, and the apparent activation energy (E_a) of the decompositions have also been calculated, and the results indicate that the main decomposition of **L** needs higher apparent activation energy values E_a than that of **1**. The acetate binding properties of **L** in solution have also been evaluated by Ultraviolet-Visible (UV-Vis) spectroscopy. CCDC: 1506202, **L**; 1506203, **1**.

Keywords: Anions, Hydrogen bonds, Pyridyl urea, Zn(II) complex, Thermal stability

Anion complexation by synthetic receptors is a significant and contemporary aspect of supramolecular chemistry due to the biological and environmental relevance[1-4]. The anion complexation is particularly challenging, compared to cationic or neutral guests, due to a large free energy of hydration and weak interaction[5]. A promising approach for anion complexation is the construction of coordination complex anion host, in which the metal salt can self-assemble with ligands containing both hydrogen bonding and Lewis basic functionality[6]. Such labile host systems can be advantageous, because the presence of certain guest species may template the formation of the host and stabilize the self-assembled complex[7]. A number of such metal-ligand architectures have been constructed to complex anions[8,9]. Viewing from the driving forces, anion hydrogen bonding interaction is one of the most efficient and key forces to stabilize these self-assembled architectures[10]. Once the anion directly participates in the coordination to the metal ion, the directionality, steric constraints and polarization of the M–A bond places considerable constraints on complexed anion hydrogen bonded geometries[11]. Hence such constraints must be understood in the design of metal salt ion pair binding hosts. The investigation of hydrogen bonding interactions to metal-coordinated anions is particularly challenging due to the constraints of geometry, strength and directionality[12].

Urea is well-known in its ability to interact well with anions as hydrogen bond donor and/or acceptor, while the pyridyl function can coordinate with metal ions[13]. Thus, urea-based pyridyl ligands have the potential of simultaneously binding metal ions and forming hydrogen bonds with anions[14]. Over the past decades, there have been various examples of metal ion directed anion complexation with ureidopyridyl ligands, including mono-pyridyl urea[15,16], bis-pyridyl ureas[17] and tris-pyridyl ureas[18], and the anion hydrogen bonding interactions were investigated in different ways[19]. However, it is still far away from understanding, regulating and controlling the interactive nature, especially for the oxo-anions such as acetate anion. In order to explore the acetate hydrogen bonding interactions in specific conditions, we designed and synthesized a pyridine-containing urea ligand,

N-(4-chlorophenyl)-*N'*-(4-pyridyl)urea (**L**) (Scheme 1), and carried out the reaction of the ligand with Zinc(II) acetate. Here, we report the supramolecular structures of the ligand **L** and the Zinc(II) acetate complex $[ZnL_2(OAc)_2]\cdot 2H_2O$ (**1**) based on different hydrogen bonding interactions, as well as the thermal stabilities and acetate binding properties of **L** and acetate complex **1**.

Experimental

Materials and instruments

All solvents for the syntheses (analytical grade) were used without further purification, and the metal salts ($Zn(OAc)_2\cdot 2H_2O$), *p*-chloro-phenylisocyanate and *p*-pyridyl-amine were commercially available. ^{1}H NMR spectra were recorded on a Bruker 600 MHz spectrometer using tetramethylsilane (TMS) as an internal standard. IR spectra were measured with an IR Spectrometer equipped with a Smart Omni-Transmission accessory (thermo Scientific). TGA/DTG data were measured by using Universal V4.4A TA Instruments under nitrogen atmosphere. The UV-Vis spectra were measured in acetonitrile solution by PERSEE TU-1950 Ultraviolet-Visible Spectrophotometer.

Synthesis

Synthesis of the ligand L

An acetonitrile solution (50 mL) of *p*-chloro-phenylisocyanate (1.53 g, 0.01 mol) was dropped into an acetonitrile solution (100 mL) of *p*-pyridyl-amine (0.94 g, 0.01 mol). The mixture was refluxed for 2 h and the precipitate thus obtained was filtered off and washed with acetonitrile and diethyl ether, and then dried over vacuum to yield **L** as a white solid (1.88 g, 76%). The crystals for detection were grown by slow evaporation from a solution of **L** in methanol/water (10:1 v/v, 5 mL) at room temperature for several days. M.P.: 234–235 °C. IR (KBr, ν/cm^{-1}): 3291 (N−H), 3061, 1726 (C=O), 1594, 1546, 1518, 1496, 1288, 1198, 822, 684. ^{1}H NMR (DMSO-d_6, 400 MHz, δ ppm): 9.16 (s, 1H, NH), 9.02 (s, 1H, NH), 8.36 (d, 2H, J = 4.0 Hz, Py-H2, Py-H6), 7.50 (d, 2H, J = 8.0 Hz, Ar-H3, Ar-H5), 7.43 (d, 2H, J = 4.0 Hz, Py-H3, Py-H5), 7.35 (d, 2H, J = 8.0 Hz, Ar-H2, Ar-H6).

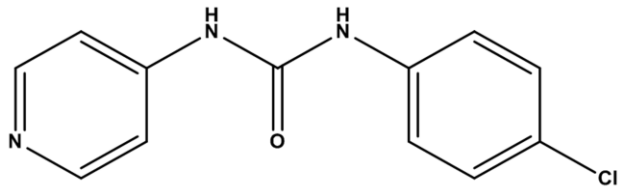

Molecular structure of **L**
Scheme 1

Synthesis of the acetate complex 1

$[ZnL_2(OAc)_2]\cdot 2H_2O$ (**1**): **L** (49.5 mg, 0.20 mmol) and $Zn(OAc)_2\cdot 2H_2O$ (21.9 mg, 0.10 mmol) were stirred in methanol/water (10:1 v/v, 11 mL) for 2 h at refluxing temperature. After cooling to room temperature, the mixture was filtered, and the filtrate was allowed to evaporate for several days to give colorless block crystals. Yield: 52%. M.P.: 206–207 °C. IR (KBr, ν/cm^{-1}): 3534 (water), 3353 (N−H), 3270 (N−H), 3082, 1740 (C=O), 1712 (C=O), 1615 (acetate), 1601, 1552, 1517, 1490, 1407 (acetate), 1295, 1191, 836, 698. ^{1}H NMR (DMSO-d_6, 600 MHz, δ ppm): 9.61 (s, 1H, NH), 9.32 (s, 1H, NH), 8.40 (br, 2H, Py-H2, Py-H6), 7.55 (br, 2H, Py-H3, Py-H5), 7.51 (d, 2H, J = 9.0 Hz, Ar-H3, Ar-H5), 7.35 (d, 2H, J = 9.0 Hz, , Ar-H2, Ar-H6), 1.85 (s, 3H, CH_3COO).

X-ray crystallography

Diffraction data for **L** and **1** were collected on a Bruker SMART APEX II diffractometer with graphite-monochromated Mo Kα radiation (λ = 0.71073 Å). The structure was solved by direct methods using the SHELXTL program package[20]. All non-hydrogen atoms were refined anisotropically by full-matrix least-squares on F^2 by the use of the program SHELXL-2018, and hydrogen atoms were included in idealized positions with thermal parameters equivalent to 1.2 times those of the atom to which they were attached. Crystallographic data for **L** and **1** are listed in Table 1.

Results and Discussion

Synthesis and formulation

Synthesis and formulation of the ligand L

The ligand **L** was readily synthesized by the reaction of *p*-chloro-phenylisocyanate with *p*-pyridyl-amine which were both commercially available. The nuclear magnetic resonance spectroscopy (^{1}H NMR) and infrared spectroscopy (IR) studies indicated that the ligand of **L** was successfully synthesized. As shown in the ^{1}H NMR spectrum of the ligand **L** (Supplementary Data, Fig. S1), the peaks of 9.16 ppm and 9.02 ppm belong to the active hydrogens on urea NH groups and the peaks of 8.36 ppm are the two protons adjacent to N on the pyridine ring. In the meantime, the peaks of 7.50 ppm are derived from the benzene ring proton adjacent to NH on the benzene

Table 1 — Crystallographic data and refinement details for compounds **L** and **1**

Compound	**L**	**1**
Empirical formula	$C_{12}H_{10}ClN_3O$	$C_{28}H_{30}Cl_2N_6O_8Zn$
Fw	247.68	714.85
Temperature / K	296(2)	296(2)
Crystal system	monoclinic	triclinic
Space group	$P2_1/n$	$P\bar{1}$
a /Å	6.979(2)	8.3860(15)
b /Å	12.808(4)	11.566(2)
c /Å	12.546(4)	17.946(3)
α /°	90.00	95.217(3)
β /°	94.201(6)	99.287(3)
γ /°	90.00	108.003(3)
V /Å^3	1118.4(7)	1615.1(5)
Z	4	2
D_{calc} /g cm^{-3}	1.471	1.470
F (000)	512	736
μ /mm^{-1}	0.327	0.982
θ range	2.275–25.099	2.326–25.099
Reflns collected	5433	8121
Independent reflns	1995	5688
Observed reflns [$I > 2\sigma(I)$]	1442	4564
R(int)	0.0337	0.0177
R_1; wR_2 [$I > 2\sigma(I)$]	0.0475; 0.1242	0.0395; 0.1045
R_1; wR_2 (all data)	0.0701; 0.1508	0.0522; 0.1119
GOF (F^2)	1.089	1.052

ring. Moreover, the remaining peaks of 7.43 ppm and 7.35 ppm are derived from the other two protons on the pyridine ring and the benzene ring, respectively. In the IR spectrum of the ligand **L**, the urea NH stretching frequency at 3291cm^{-1} and the carbonyl C=O stretching vibration at 1726 cm^{-1} clearly indicate the presence of the urea group. Furthermore, the aromatic ring C-H stretching vibration at 3061 cm^{-1} and C=C contraction vibrations at 1594 cm^{-1}, 1546 cm^{-1}, 1518 cm^{-1} and 1496 cm^{-1} indicated the presence of the aromatic rings.

Synthesis and formulation of the complex [ZnL$_2$(OAc)$_2$]·2H$_2$O (1)

Reaction of $Zn(OAc)_2·2H_2O$ with 2 equivalents of **L** in methanol/water afforded the complex $[ZnL_2(OAc)_2]·2H_2O$ (**1**), as determined by the NMR and IR analysis. As shown in the ^{1}H NMR spectrum of the complex **1** (Supplementary Data, Fig. S2), the shifts of NH (9.61 ppm, 9.32 ppm) in complex **1** are remarkably downfield shifts in contrast to that of ligand **L** (9.16 ppm, 9.02 ppm), thus implying that the NH groups in the complex **1** take part in stronger hydrogen bonding interactions than that of NH groups in the ligand **L**. Furthermore, the peaks of Py-H in the complex **1** are also observed downfield shifts relative to that of the ligand **L**. Notably, the shift of acetate (1.85 ppm) could be observed in the NMR spectrum of the complex **1**, indicating the presence of acetate anion in the complex **1**. In the IR spectrum of the complex **1**, the vibration frequency at 3534 cm^{-1} suggested the presence of water molecules. The IR spectrum of the complex **1** is consistent with the hydrogen bond formation. The urea NH stretch frequencies at 3353 cm^{-1} and 3270 cm^{-1} in complex **1** are different from that of **L** (3291 cm^{-1}), which may be attributed to the different hydrogen bond types. The C=O stretching frequencies at 1740 cm^{-1} and 1712 cm^{-1} belong to the carbonyl groups of urea (-NHCONH-) and the frequency at 1615 cm^{-1} could be attributed to the carboxyl group of acetate (CH_3COO-), respectively.

Description of crystal structures

Crystal structure of the ligand L

The ligand **L** crystallizes in the monoclinic space group $P2_1/n$ in the self-association mode. In this structure, **L** displays a slightly twisted conformation wherein the two aryl rings make a dihedral angle of 11.11°. Although the chlorophenyl moiety is almost coplanar with the urea carbonyl (torsion angle $C6_{urea}$–N3–$C7_{chlorophenyl}$–C8 0.9(4)°), the pyridyl ring lies in a slightly twisted position relative to the chlorophenyl–urea plane, with a torsion angle of 11.9(4)° ($C6_{urea}$–N2–$C3_{py}$–C2) (Fig. 1). The urea NH

groups form two intermolecular N–H···N hydrogen bonds (N2–H2···N1^{i}: N2···N1^{i}, 3.199(3) Å, ∠N2–H2···N1^{i}, 148.9°; N3–H3···N1^{i}: N3···N1^{i}, 3.066(3) Å, ∠N3–H3···N1^{i}, 152.1°) with a pyridyl nitrogen acceptor of another molecule with an $R_2^1(6)$ motif[21], leading to the formation of 1-D zigzag urea-pyridyl tape hydrogen bonding network (Fig. 2). Obviously, the urea N–H···$N_{pyridyl}$ interaction tape is different from the typical urea N–H···O_{urea} tape α-network as in many substituted ureas[22]. Moreover, the 1-D zigzag hydrogen bond chains are further self-assembled via C–H···O interactions (C9···O1^{ii}, 3.328(4) Å, ∠C9–H9···O1^{ii}, 149.7°) involving carbonyl oxygen atom of urea functionality and aromatic hydrogen of neighbouring chains. As a result, such 1-D hydrogen bonded chains are further arranged in 2-D sheetlike network structure sustained by the above mentioned C–H···O interactions (Fig. 3). The hydrogen bond parameters for **L**, as well as for Zinc(II) acetate complex **1**, are summarized in Table 2.

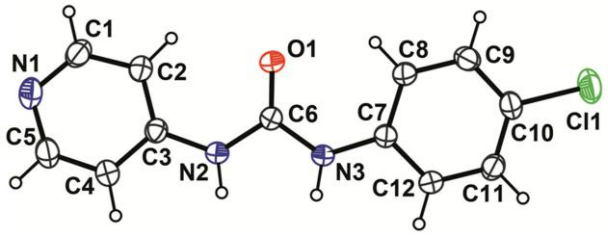

Fig. 1 — Molecular structure of the free ligand L (thermal ellipsoid at 30% probability level).

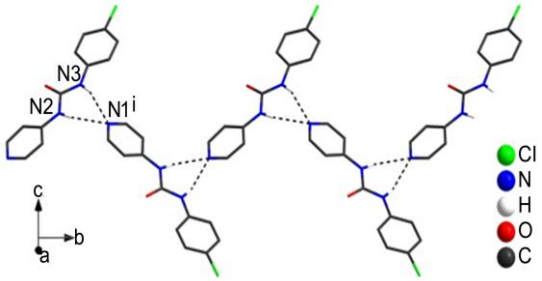

Fig. 2 — 1-D zigzag hydrogen bonding chain of L self-assembled by the urea N–H···$N_{pyridyl}$ interactions. Hydrogen atoms not involved in these interactions are omitted for clarity. Symmetry codes: ^{i} 2.5−*x*, 0.5+*y*, 0.5−*z*.

Crystal structure of the complex [ZnL$_2$(OAc)$_2$]·2H$_2$O (1)

The Zinc(II) acetate complex **1** is prepared by reacting **L** and $Zn(OAc)_2·H_2O$ (2:1 molar ratio) in MeOH/H_2O. **1** crystallizes in the triclinic space group $P\bar{1}$. The asymmetric unit contains two ligands **L**, two acetate anions–all coordinated to the metal center Zn(II), and two crystal water molecules (Fig. 4).

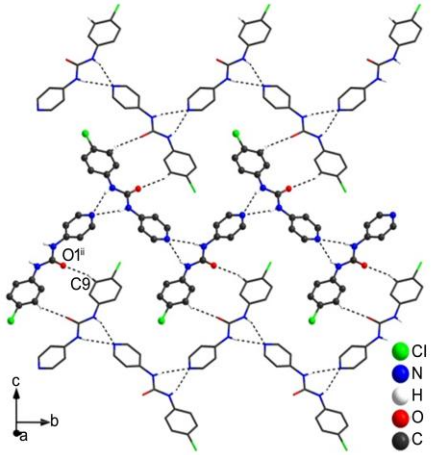

Fig. 3 — 2-D sheetlike network structure of L sustained by the urea N–H···$N_{pyridyl}$ interactions and C–H···O interactions. Hydrogen atoms not involved in these interactions are omitted for clarity. Symmetry codes: ^{ii} 1−*x*, −*y*, 1−*z*.

Table 2 — Selected hydrogen bond parameters (Å, °) for **L** and **1**

Compound	D–H···A	D–H (Å)	H···A (Å)	D···A (Å)	∠D–H···A (°)
L	N2–H2···N1^{i}	0.86	2.43	3.199(3)	148.9
	N3–H3···N1^{i}	0.86	2.28	3.066(3)	152.1
	C9–H9···O1^{ii}	0.93	2.49	3.328(4)	149.7
1	N2–H2···O6^{i}	0.86	1.96	2.819(3)	174.7
	N3–H3···O7^{ii}	0.86	2.15	2.883(4)	142.6
	N5–H5···O8^{iii}	0.86	2.04	2.856(3)	159.0
	N6–H6···O8^{iii}	0.86	2.12	2.931(4)	156.3
	O7–H7A···O1	0.82(6)	2.05(6)	2.844(4)	161(6)
	O7–H7···O3^{iv}	0.75(6)	2.11(6)	2.860(4)	172(6)
	O8–H8A···O4^{iv}	0.83(5)	1.93(5)	2.747(4)	170(4)
	O8–H8B···O5^{v}	0.74(4)	2.07(4)	2.781(4)	162(4)
	C12–H12···O7^{ii}	0.93	2.57	3.185(5)	124.4

Symmetry codes for **L**: ^{i} 2.5−*x*, 0.5+*y*, 0.5−*z*; ^{ii} 1−*x*, −*y*, 1−*z*. Symmetry codes for **1**: ^{i} −*x*, −*y*+2, −*z*; ^{ii} −*x*, −*y*+1, −*z*; ^{iii} 1−*x*, 1−*y*, 1−*z*; ^{iv} *x*, *y*−1, *z*; ^{v} *x*+1, *y*−1, *z*.

In this structure, **L** displays a slightly twisted conformation wherein the two aryl rings make dihedral angles of 7.04° and 8.10°, respectively, indicating no obvious change in conformation relative to the free ligand. The metal center Zn(II) displays a four-coordinated geometry considering only one coordinated oxygen atom of both of the acetate anions, respectively. The coordinating distances Zn–N are 2.037(2) Å and 2.047(2) Å, whereas the Zn–O distances vary from 1.939(2)–1.988(2) Å (Table 3), which are slightly shorter than the Zn–O distances (1.972(5)–2.488(5) Å) involved acetate anion reported previously by Das *et al.*[23] The coordinating angles involved metal center Zn(II) vary from 96.87(9)° to 128.07(10)°, and the two largest angles O−Zn−N in the four-coordinate species are 128.07(10) and 117.51(9), respectively. According to the four-coordinate geometry index (τ4) established by Houser *et al.*,[24] the coordination geometry about the Zn atom is distorted tetrahedral, with a τ4 value of 0.81 (the value of τ4 ranges from 1.00 for a perfect tetrahedral geometry, to zero for a perfect square planar geometry, while intermediate structures, including trigonal pyramidal and seesaw, fall within the range of 0 to 1.00).

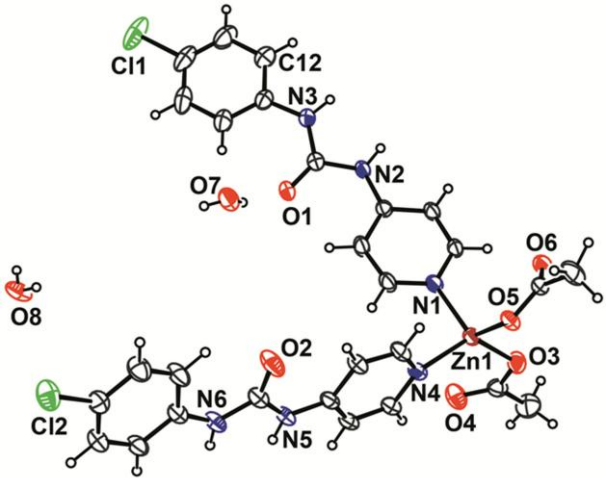

Fig. 4 — Molecular structure of $[ZnL_2(OAc)_2]\cdot 2H_2O$ (1) showing the coordination geometry of the Zn^{2+} center (thermal ellipsoid at 30% probability level).

The two ligand arms of each $[ZnL_2(OAc)_2]\cdot 2H_2O$ unit participate in intermolecular contacts with adjacent molecules. The urea NH groups of one ligand form two N−H···O hydrogen bonds with acetate moiety of another molecule (N2···O6^{i}, 2.819(3) Å, ∠N2–H2···O6^{i}, 174.7°) and one of the two bound water molecules within the structure (N3···O7^{ii}, 2.883(4) Å, ∠N3–H3···O7^{ii}, 142.6°). This water molecule itself donates an O–H···O hydrogen bond to another acetate moiety of the above mentioned another molecule. Moreover, the other ligand of the same $[ZnL_2(OAc)_2]\cdot 2H_2O$ unit donates two N−H···O hydrogen bonds to the second water molecule with an $R_2^1(6)$ motif(N5–H5···O8^{iii}: N5···O8^{iii}, 2.856(3) Å, ∠N5–H5···O8^{iii}, 159.0°; N6–H6···O8^{iii}: N6···O8^{iii}, 2.931(4) Å, ∠N6–H6···O8^{iii}, 156.3°), and the bridged water molecule itself also donates an O−H···O hydrogen bond to oxygen atom of acetate anion come from the third $[ZnL_2\ (OAc)_2]\cdot 2H_2O$ molecule. These hydrogen bonds further expand $[ZnL_2(OAc)_2]\cdot 2H_2O$ units to generate one dimensional hydrogen bonded chains, as seen in Fig. 5. Interestingly, the water-bridged hydrogen

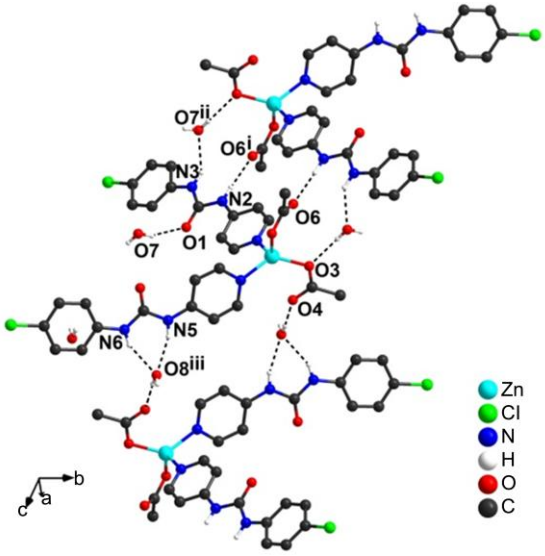

Fig. 5 — 1-D hydrogen bonded chain of 1 generated by N−H···O and O−H···O hydrogen bonds. Hydrogen atoms not involved in these interactions are omitted for clarity. Symmetry codes: ^{i} $-x$, $-y+2$, $-z$; ^{ii} $-x$, $-y+1$, $-z$; ^{iii} $1-x$, $1-y$, $1-z$.

Table 3 — Selected bond lengths (Å) and angles (°) for **1**

Bond	Dist.	Bond	Angle
Zn1–N1	2.037(2)	O3−Zn1−N4	128.07(10)
Zn1−N4	2.047(2)	O5−Zn1−N1	117.51(9)
Zn1−O3	1.939(2)	O3−Zn1−N1	111.05(10)
Zn1−O5	1.988(2)	O3−Zn1−O5	103.87(9)
O3−C27	1.270(4)	N1−Zn1−N4	99.85(9)
O5− C25	1.284(3)	O5−Zn1−N4	96.87(9)

bonded network is different from the typical urea N−H···O_{urea} tape α-network as in many diarylureas,[22] and is also different from the urea N−H···$N_{pyridyl}$ interaction tape observed in the structure of the same free ligand **L**. The urea N−H···$N_{pyridyl}$ interaction is 'switched off' by metal coordination in the Zinc(II) acetate complex.

One of the two enclathrated water molecules donates two O−H···O hydrogen bond to an oxygen atom of one carbonyl group of a ligand arm (O7···O1, 2.844(4) Å, ∠O7–H7A···O1, 161(6)°) and to an oxygen atom of one of the acetate anion moiety come from neighboring 1-D hydrogen bonded chains (O7···O3^{iv}, 2.860(4) Å, ∠O7–H7···O3^{iv}, 172(6)°), which expand the 1-D hydrogen bonded chains to 2-D sheetlike structure (Fig. 6). The 2-D sheetlike structures are further extended to 3-D hydrogen bonded network sustained by O−H···O hydrogen bond interactions involving oxygen atom of the other bridged water molecule and two acetate anion moieties come from neighbouring different 2-D sheetlike structures (O8–H8A···O4^{iv}: O8···O4^{iv}, 2.747(4) Å, ∠O8–H8A···O4^{iv}, 170(4)°; O8–H8B···O5^{v}: O8···O5^{v}, 2.781(4) Å, ∠O8–H8B···O5^{v}, 162(4)°). The weak intermolecular C–H···O interaction (C12··· O7^{ii}, 3.185(5) Å, ∠C12–H12···O7^{ii}, 124.4°) involving oxygen atom of bound water molecule and aromatic hydrogen is also observed.

The hydrogen bonds involving acetate anion is shown as Fig. 7. The coordinated oxygen atoms of acetate (O3 and O5) receive an O−H···O hydrogen bond from one of the two enclathrated water molecules, respectively. The non-coordinated oxygen atoms of acetate receive an O−H···O hydrogen bond (for O4) from one of the two enclathrated water molecules and a N−H···O hydrogen bond (for O6) involving the urea NH group of the ligand. The enclathrated water molecules act as hydrogen bonding donors and accepters at the same time. These hydrogen bonds involving acetate anions and the bridged water molecules play an important role in stabilizing the supramolecular structures.

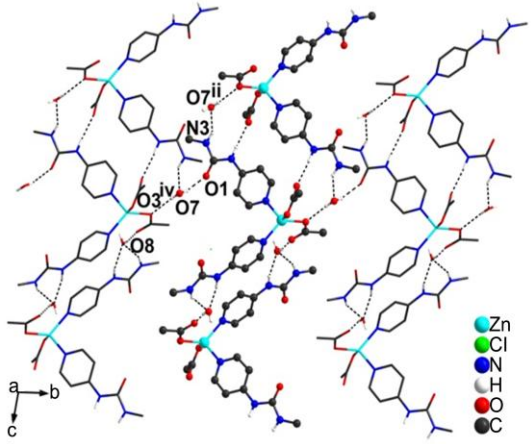

Fig. 6 — 2-D sheetlike structures of 1 linked by intermolecular N−H···O and O−H···O hydrogen bonds involving urea groups, acetate anions and bridged water molecules. Partial atoms not involved in these interactions are omitted for clarity. Symmetry codes: [ii] −*x*, −*y*+1, −*z*; [iv] *x*, *y*−1, *z*.

Thermal Analyses

Thermal decomposition processes of L and 1 under nitrogen

To estimate the stability of the ligand **L** and the complex **1**, thermogravimetric analyses experiments were carried out in the temperature range of 30–1000 °C. The TGA curves of the ligand **L** and the complex **1** under nitrogen at the heating rate of 5 °C min^{-1} are represented in Fig. 8. The DTG curves of the ligand **L** and the complex **1** under nitrogen at

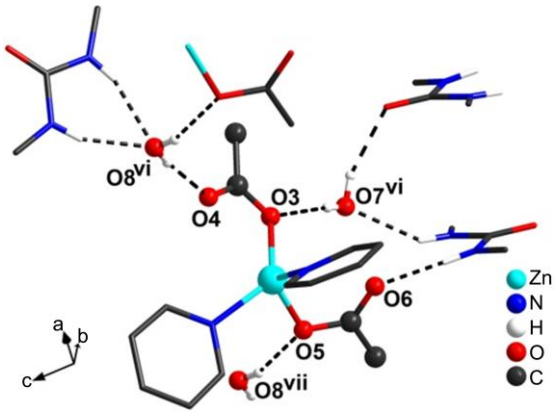

Fig. 7 — Hydrogen bonding interactions around the acetate anion in 1. Symmetry codes: [vi] *x*, 1+*y*, *z*; [vii] *x*−1, 1+*y*, *z*.

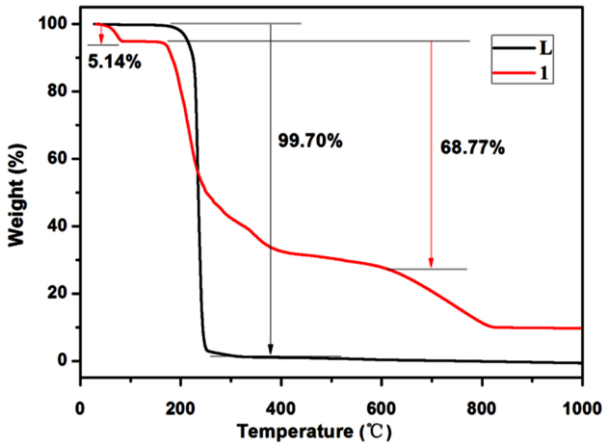

Fig. 8 — TGA curves of the ligand **L** (black) and the complex **1** (red) at a heating rate of 5 °C min^{-1} under nitrogen condition.

the heating rate of 5, 10 and 15 °C min^{-1} are shown in Fig. 9 and Fig. 10, respectively.

The ligand **L** undergoes one stage of rapid weight loss during 30–1000 °C, and the endothermic peak is in the temperature of 234.53 °C at the heating rate of 5 °C min^{-1}, as shown in Fig. 8 and 9. The value of the weight loss at this stage is 99.70%, which is attributed to the complete decomposition of the ligand molecule, as shown in Fig. 8.

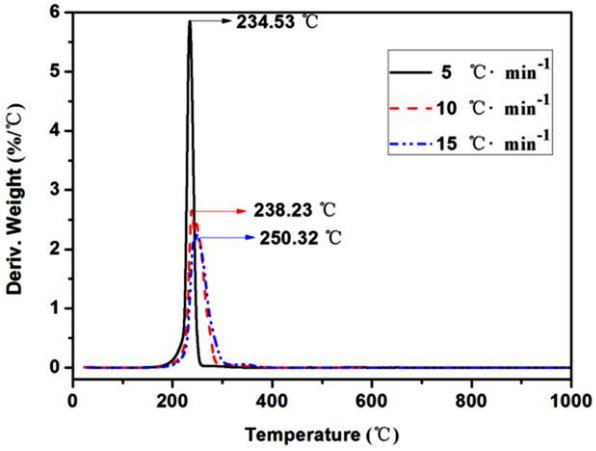

Fig. 9 — DTG curves of the ligand **L** at the heating rate of 5, 10 and 15 °C·min^{-1} under nitrogen condition.

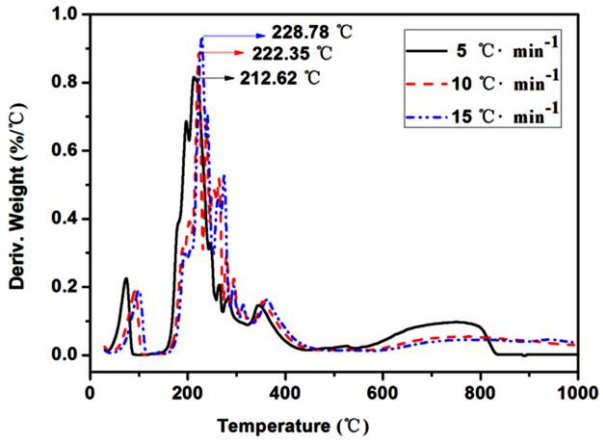

Fig. 10 — DTG curves of the complex **1** at the heating rate of 5, 10 and 15 °C·min^{-1} under nitrogen condition.

It can be seen from Fig. 8 and Fig. 10, two stages of weight loss of the complex **1** can be clearly discerned under the heating rate of 5 °C min^{-1}. The first step starts from 60 °C and ends at 80 °C with the sum loss of 5.14% which should be assigned to two enclathrated water molecules (Calcd. 5.04%). The second step starts from 169 °C and remains level at 613 °C. In this temperature region, the sum of weight loss is 68.77%, which should be possibly assigned to the decomposition of the two coordinated ligand molecules in complex **1** (Calcd. 69.30%).

Kinetic calculation

By substituting the different heating rate (β) and corresponding peak temperature value (T_p) on DTG curve into Kissinger formula (1) and Ozawa[25–29] formula (2), the apparent activation energy values E_a and the pre-exponential factor A could be calculated by linear fitting in the computer. The kinetic parameters of main decomposition processes for the ligand **L** and the complex **1** under nitrogen obtained by methods of Kissinger and Ozawa are listed in Table 4, and the experimental results indicate that the main decomposition of the ligand **L** needs higher apparent activation energy values E_a than that of **1**.

$$\ln\left(\frac{\beta}{T_p^{\,2}}\right)=\ln\left(\frac{AR}{E_a}\right)-\frac{E_a}{RT_p} \quad \text{(Kissinger)} \qquad \ldots(1)$$

$$\lg\beta=\lg\left[\frac{AE_a}{RG(\alpha)}\right]-2.315-0.4567\frac{E_a}{RT_p} \quad \text{(Ozawa)} \qquad \ldots(2)$$

Where, β is the different heating rate, T_p is the corresponding peak temperature value on DTG curve, A is the pre-exponential factor, R is the gas constant, E_a is the apparent activation energy value, and $G(\alpha)$ is the mechanism function. According to Kissinger formula (1), the linear plot of $\ln(\beta/T_p^{\,2})$ versus $1/T_p$ enables E_a and A to be determined from the slope and the intercept respectively. For the Ozawa formula (2), due to the

Table 4 — Kinetic parameters of the main thermal decomposition process of **L** and **1** under nitrogen condition.

Complex	β/ °C min^{-1}	T_p / °C	Kissinger			Ozawa	
			E_a/ kJ mol^{-1}	lg$A$	R^2	E_a/ kJ mol^{-1}	R^2
	5.00	234.53					
L	10.00	238.23	146.0	14.5	0.9933	147.0	0.9941
	15.00	250.32					
	5.00	212.62					
1	10.00	222.35	130.0	13.5	0.9987	131.4	0.9989
	15.00	228.78					

unknown $G(\alpha)$, the value of E_a can be calculated using formula (2) from the slope of the plot of lgβ versus $1/T_p$.

Acetate binding properties of L

Acetate binding mode

The acetate binding of L in solution was evaluated by UV-Vis studies of L with addition of Ac^- (in the form of Tetrabutylammonium acetate). The Job's plots[30,31] of UV spectroscopy suggested that the apparent stoichiometry ratio of L to Ac^- is 1:1 in acetonitrile solution (Fig. 11).

$$[HG] = [H] \bullet \frac{A_0 - A}{A_0} \quad \ldots(3)$$

Where, [HG] is the concentration of the complex, and [H] is the corresponding ligand concentration. When A_0 is the absorbance of a pure ligand, A is the absorbance of L after adding an anion. From the stoichiometry ratio obtained, the association constant K between L and acetate can be calculated from the titration of UV spectroscopy.

Acetate binding constant

When acetate ions were added to the solution of L, a red shift was observed from 266 nm to 274 nm with an isosbestic point at 264 nm (Fig. 12a). This shows that there is a stable complex formation. As demonstrated in the Job's plot in Fig.11, the binding mode of L with Ac^- is 1:1. According to the change in absorbance at 274 nm (Fig. 12b), the binding constant of the ligand to acetate was K = 5.74×10^5 M^{-1} (R = 0.995) using the nonlinear fit[32-34] using Equation 4.

$$A = A_0 + \frac{A_{limit} - A_0}{2C_0}\left[x + c_0 + 1/K - \sqrt{(x + c_0 + 1/K_a)^2 - 4c_0 x}\right] \quad \ldots(4)$$

Where, A_0 is the absorbance of the ligand at 274 nm, A and A_{limit} are the absorbance of the solution after adding anion at this wavelength and its limit value, c_0 is the initial molar concentration of the ligand, K is the binding constant of ligand to acetate, and x is the molar concentration of anions during the titration.

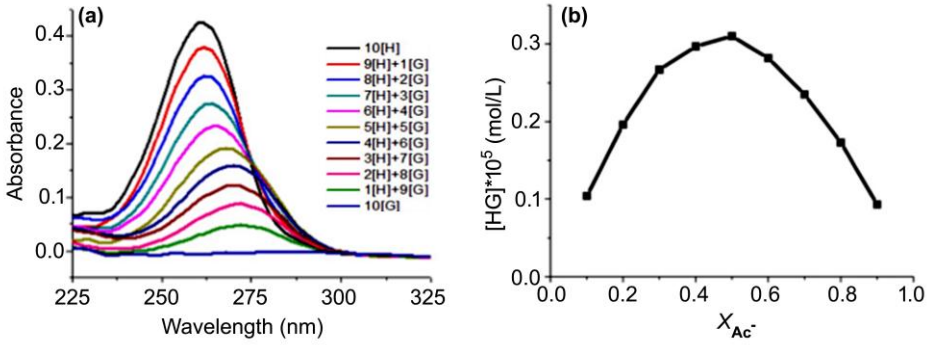

Fig. 11 — a) UV-Vis spectra of complexation of L with Ac^- in acetonitrile at room temperature, H = L, G = Ac^- (TBAAc), [10H] = [10G] = 10^{-5} M. b) Job's plot of molar fraction X_{Ac^-} versus the [HG] at 260 nm, X_{Ac^-} is the molar fraction of Ac^-.

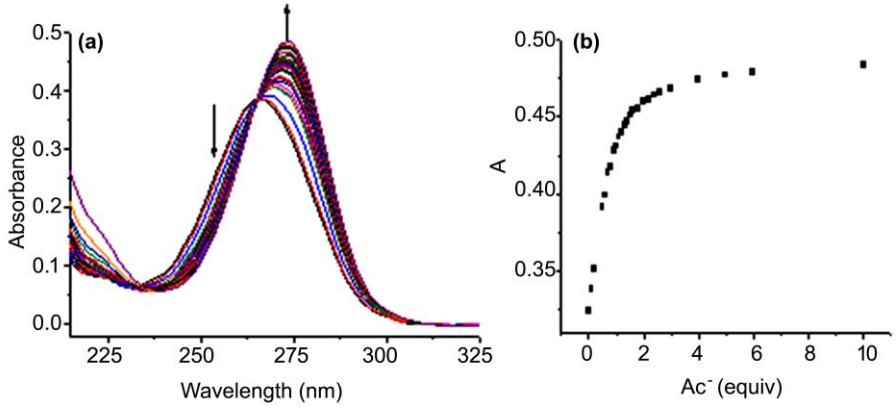

Fig. 12 — a) UV-Vis spectra of L (10^{-5} M in acetonitrile) upon addition of 0–10 equiv of Ac^- at room temperature. b) The increase of absorbance at 274 nm.

Conclusions

In conclusion, we report the supramolecular structures of a urea-based pyridyl ligand **L** and its zinc(II) acetate complex **1**. The free ligand **L** displays 2-D sheetlike network structure formed by the urea N−H···$N_{pyridyl}$ interactions and C–H···O interactions. However, in the complex **1**, the urea N−H···$N_{pyridyl}$ interaction is 'switched off' by metal coordination. Complex **1** presents 3-D hydrogen bonded network formed by intermolecular N−H···O and O−H···O hydrogen bonds involving urea groups, acetate anions and bridged water molecules. The thermal stabilities of **L** and **1** are investigated, and the apparent activation energy (E_a) of the decompositions are also calculated, and the results indicate that the main decomposition of **L** needs higher apparent activation energy values E_a than that of **1**. Job plot experiment shows that the binding mode of L with Ac^- is 1:1, and the UV-Vis spectra titration indicates that the binding constant (K) of the ligand to acetate is 5.74×10^5 M^{-1}.

Supplementary Data

CCDC 1506202 for **L** and 1506203 for **1** contain the supplementary crystallographic data (CIF) for this paper. These data can be obtained free of charge via http://www.ccdc.cam.ac.ukconts/ retrieving.html (or from the Cambridge Crystallographic Data Centre, 12, Union Road, Cambridge CB2 1EZ, UK; fax: +44-1223-336-033). Supplementary Data associated with this article are available in the electronic form at http://www.niscair.res.in/jinfo/ijca/IJCA_58A(12)1302-1310_SupplData.pdf.

Acknowledgement

The work was supported by the National Natural Science Foundation of China (No. 21301139, 21073139, 21103135, 21701131), China Scholarship Council (No. 201808615050), the Youth Innovation Team of Shaanxi Universities, Natural Science Basic Research Plan in Shaanxi Province of China (No.2015JQ2043) and the Undergraduate Innovation and Entrepreneurship Training Program in Shaanxi Province of China (No. 201510704057).

References

1 Bowman-James K, *Acc Chem Res*, 38 (2005) 671.
2 Gale P A & Quesada R, *Coord Chem Rev*, 250 (2006) 3219.
3 Mullen K M & Beer P D, *Chem Soc Rev*, 38 (2009) 1701.
4 Steed J W, *Chem Soc Rev*, 38 (2009) 506.
5 Bianchi A, Bowman-James K & Garcia-Espana E, *Supramolecular Chemistry of Anions*, Wiley-VCH, New York, 1997.
6 Applegarth L, Goeta A E & Steed J W, *Chem Commun*, (2005) 2405.
7 Turner D R, Smith B, Spencer E C, Goeta A E, Evans I R, Tocher D A, Howard J A K & Steed J W, *New J Chem*, 29 (2005) 90.
8 Bondy C R, Gale P A & Loeb S J, *J Am Chem Soc*, 126 (2004) 5030.
9 Huang X, Yang Z, Yang X-J, Zhao Q, Xia Y & Wu B, *Inorg Chem Commun*, 13 (2010) 1103.
10 Turner D R, Hursthouse M B, Light M E & Steed J W, *Chem Commun*, (2004) 1354.
11 Qureshi N, Yufit D S, Steed K M, Howard J A K & Steed J W, *CrystEngComm*, 18 (2016) 5333.
12 Byrne P, Lloyd G O, Applegarth L, Anderson K M, Clarke N & Steed J W, *New J Chem*, 34 (2010) 2261.
13 Turner D R, Henry M, Wilkinson C, McIntyre G J, Mason S A, Goeta A E & Steed J W, *J Am Chem Soc*, 127 (2005) 11063.
14 Jia C, Zuo W, Zhang D, Yang X-J & Wu B, *Chem Commun*, 52 (2016) 9614.
15 Yang Z, Wu B, Huang X, Liu Y, Li S, Xia Y, Jia C & Yang X-J, *Chem Commun*, 47 (2011) 2880.
16 Yang Z, Huang X, Zhao Q, Li S & Wu B, *CrystEngComm*, 14 (2012) 5446.
17 Custelcean R, Sellin V & Moyer B A, *Chem Commun*, (2007) 1541.
18 Wu B, Liang J, Yang J, Jia C, Yang X-J, Zhang H, Tang N & Janiak C, *Chem Commun*, (2008) 1762.
19 Ravikumar I & Ghosh P, *Chem Soc Rev*, 41 (2012) 3077.
20 Sheldrick G M, *Acta Cryst*, C71 (2015) 3.
21 Etter M C, *Acc Chem Res*, 23 (1990) 120.
22 Etter M C, Urbanczyk-Lipkowska Z, Zia-Ebrahimi M & Panunto T W, *J Am Chem Soc*, 112 (1990) 8415.
23 Kumar D K, Das A & Dastidar P, *CrystEngComm*, 8 (2006) 805.
24 Yang L, Powell D R & Houser R P, *Dalton Trans*, 9 (2007) 955.
25 Hu R Z, Gao S L, Zhao F Q, Shi Q Z, Zhang T L & Zhang J J, *Thermal Analysis Kinetics*, (Science Press, Beijing) 2008, p. 79.
26 Yang Z, Ding Z, Liu X, Zhao S, Zhang R & Yang S, *Chin J Inorg Chem*, 31 (2015) 1520.
27 Yang Z, Liu X, Zhao S & He J, *Prog Chem*, 26 (2014) 1899.
28 Ren J, Liu X, Yang Z & Zhao S, *Thermochim Acta*, 582 (2014) 17.
29 Yang Z, Liu X, Bai X, Zhao S, Yang Z & Qu M, *Mol Cryst Liq Cryst*, 658 (2017), 177.
30 Kim J S, Shon O J, Yang S H, Kim J Y & Kim M J, *J Org Chem*, 67 (2002) 6514.
31 Tatsuya M, Hisafumi H & Hiroshi N, *Chem Lett*, 32 (2003) 146.
32 Connors K A, *Eur J Med Chem*, 22 (1987) 373.
33 Bourson J, Pouget J & Valeur B, *J Phys Chem*, 97 (1993) 4552.
34 Valeur B, Pouget J, Bourson J, Kaschke M & Ernsting N P, *J Phys Chem*, 96 (1992) 6545.